Regenerative Therapy 3 (2016) 90–96

Contents lists available at ScienceDirect

Regenerative Therapy

journal homepage: http://www.elsevier.com/locate/reth

Original article

Heterogeneous filament network formation by myosin light chain isoforms effects on contractile energy output of single cardiomyocytes derived from human induced pluripotent stem cells

Takeomi Mizutani*, Kazuya Furusawa, Hisashi Haga, Kazushige Kawabata

Department of Advanced Transdisciplinary Sciences, Faculty of Advanced Life Science, Hokkaido University, North 10 West 8, Kita-ku, Sapporo 060-0810, Japan

ARTICLE INFO

Article history:
Received 7 December 2015
Received in revised form
19 February 2016
Accepted 22 February 2016

Keywords:
Human induced pluripotent stem cell
Cardiomyocyte
Traction force
Strain energy
Myosin II regulatory light chain
Collagen gel

ABSTRACT

Cardiomyocytes derived from human induced pluripotent stem cells (hiPSC-CMs) are expected to play an important role in heart therapies, in which hiPSC-CMs should generate sufficient contractile force to pump blood. However, recent studies have shown that the contractility of myocardial mimics composed of hiPSC-CMs is lower than that of adult human myocardium. To examine the mechanism by which contractile force output of hiPSC-CMs is weakened, we measured the contractile force of single hiPSC-CMs and observed the fibrous distribution of myosin II regulatory light chain (MRLC) of cardiac (contributes to beating) and non-cardiac (does not contribute to beating) isoforms. Single hiPSC-CMs were cultured on an extracellular matrix gel, and the contractile force and strain energy exerted on the gel were measured. Strain energy was not uniform between cells and ranged from 0.2 to 5.8 pJ. The combination of contractile force measurement and immunofluorescent microscopy for MRLC isoforms showed that cells with higher strain energy expressed the weakened non-cardiac myosin II fibers compared to those of cells with lower strain energy. Observation of cardiac and non-cardiac MRLC showed that the MRLC isoforms formed heterogeneous filament networks. These results suggest that strain energy output from single hiPSC-CMs depends both cardiac and non-cardiac myosin fibers, which prevent deformation of the cell body.

1. Introduction

Application of cardiomyocytes derived from human induced pluripotent stem cells (hiPSC-CMs) for *in vivo* repair and regenerative medicine has been examined (see review articles [1,2] and references therein). The physiological function of cardiomyocytes is to output contractile force to the extracellular matrix (ECM), where the force is sufficient to pump blood throughout the body. Schwan et al. stated that the contractile force of myocardial mimics composed of hiPSC-CMs was 10-fold lower than that of the adult human myocardium [3]. Moreover, Lu et al. repopulated hiPSC-CMs to a decellularized mouse heart, observed its beating, but found that the heart tissues was insufficient for pumping blood [4]. Thus, it is important to produce hiPSC-CMs with greater contractility. Recently, the group of Dr. Yamashita developed an efficient method for purifying hiPSC-CMs from human induced pluripotent cell derivatives [5] and demonstrated its application in infarcted hearts [6]. To expand the applications of hiPSC-CMs, contractile force and strain energy output should be examined.

Some methods for measuring the contractile force of single cardiomyocytes have been developed, including polyacrylamide hydrogel substrates with embedded beads [7,8], polydimethylsiloxane micro pillars [9], and carbon fiber tip [10]. Although hydrogel with embedded beads is advantageous for avoiding the effect of the constrained cellular adhesion area to the substrate, it is unclear whether the embedded microbeads reflect the gel surface. Thus, visualization of the polymer network itself should be conducted. Recently, covalently bonded collagen to a fluorescent dye and observed the cellular response to the collagen [11]. Since the elastic modulus of the gelled collagen was constant

Abbreviations: hiPSC-CMs, cardiomyocytes derived from human induced pluripotent stem cells; ECM, extracellular matrix; GFP, green fluorescent protein; MRLC, myosin II regulatory light chain.

* Corresponding author. Tel./fax: +81 11 706 3810.
E-mail address: mizutani@sci.hokudai.ac.jp (T. Mizutani).

Peer review under responsibility of the Japanese Society for Regenerative Medicine.

http://dx.doi.org/10.1016/j.reth.2016.02.009

for the small strain and the viscosity was negligible over the time scale of cell migration [12], fluorescent collagen gel is useful for measuring cellular contractile force.

The mechanical properties of cells are closely related to the function of myosin II. Beating contractility of cardiomyocyte depends on the cardiac isoform of myosin II [2]. Based on Hooke's law, force generated by cardiac myosin II activity balances the sum of the restoring force to the deformation of the ECM and the cell itself. Assuming that cardiac myosin II activity is constant, if the cell has higher elasticity, contractile force output to the ECM will be lower. In contrast, if the cell has lower elasticity, the contractile force output will be higher. In non-cardiac cells, cellular elasticity is highly dependent on the non-cardiac isoform of myosin II [13,14]. Taking previous studies into consideration, we hypothesized that the contractile force and strain energy output of hiPSC-CMs depend not only on cardiac myosin II but also on non-cardiac myosin II.

In this study, we measured the contractile force and strain energy output of the purified single hiPSC-CMs. The difference in the strain energy output between beating hiPSC-CMs was evaluated in terms of expression of non-cardiac myosin II. The expression of non-cardiac myosin II in hiPSC-CMs is also discussed.

2. Materials and methods

2.1. Cells culture and plasmid construction

Purified hiPSC-CMs (Cellartis Cardiomyocytes; catalogue #Y10071; source #P11012) were purchased from Takara Inc. (Shiga, Japan). Procedure of the cell culture was conducted following the manufacturer's instructions. Two weeks after cultivation, hiPSC-CMs were trypsinized and used in subsequent experiments. The human fibroblast cell line (MRC-5 SV1 TG1) was purchased from RIKEN Cell Bank (Tsukuba, Japan) and the culture protocols were used according to those described previously [15]. Transfection of a plasmid into hiPSC-CMs and MRC-5 SV1 TG1was performed using Lipofectamine 2000 (Thermo Fisher Scientific, Waltham, MA, USA).

To construct the green fluorescent protein (GFP)-tagged cardiac isoform of myosin regulatory light chain (MRLC), cDNA encoding full-length MYL2 (accession number: BC031006) was amplified by PCR, using the cDNA pool of the hiPSC-CMs, and inserted into the *Xho*I-*Kpn*I sites of pAcGFP-N3 (Takara). Primers and plasmid DNA sequences are shown in Supplementary data. GFP-MRLC expressing cells were observed by confocal laser scanning microscopy using a 63× objective lens (TCS-SP5; Leica Microsystems, Wetzlar, Germany). Beating hiPSC-CMs were observed at 512 × 512 pixels and 4 frames/s.

2.2. Preparation and mechanical properties of collagen gel

We purchased porcine-derived type I collagen solution (3 mg/mL; Cellmatrix-IP; Nitta Gelatin Inc., Osaka, Japan). The collagen was labeled with Alexa Fluor 546 according to the manufacturer's instructions (Alexa Fluor protein labeling kit; Thermo Fisher Scientific). A related method has been reported previously [16]. According to previous reports, collagen gel can be considered an elastic material under a small strain range (approximately around 0.2, depending on the experimental system) and the strain range can be widened with increasing collagen concentration [17,18]. To concentrate the collagen solution, the fluorescent-labeled collagen solution was centrifuged (Centrisart I; 20,000 MW cut off; Satorius AG, Goettingen, Germany). Collagen gelation was performed in a glass-bottom dish (8-well Nunc™ Lab-Tek™ II Chamber Slide™ System; Thermo Fisher Scientific) according to the Nitta Gelatin instructions and the final concentration of the collagen gel was 6 mg/mL. The thickness of the collagen gel was approximately 200 μm.

Prior to contractile force measurement of the gel, we evaluated Poisson's ratio and elasticity (Young's modulus) of the collagen gel. We used non-labeled collagen gel (final concentration was 6 mg/mL) in the following Poisson's ratio and the elasticity measurements assuming that the mechanical properties of the fluorescent-tagged collagen gel and non-labeled collagen gel were the same.

For Poisson's ratio measurement, we prepared a columnar collagen gel (diameter = 16 mm, height = 3 mm). The gel was transferred onto a transparent and flat-bottom vat supplied with HEPES buffered low-glucose Dulbecco's modified Eagle's medium (Sigma, St. Louis, MO, USA). We measured changes in the diameter and the height of the gel using a reading microscope with increasing load to the gel. Changes in the diameter and height were converted to longitudinal and lateral strains. Poisson's ratio was analyzed by dividing lateral strain by longitudinal strain. The averaged Poisson's ratio was 0.36 (standard deviation was 0.17, calculated from seven observations).

Measurement of collagen gel elasticity using atomic force microscopy has been previously described [19]. Briefly, a spherical bead 100 μm in diameter was indented into the collagen gel, and the force acting on the bead was recorded as a function of indentation distance. The relationship between force and distance was analyzed using the Hertzian contact theory. Averaged elasticity was 3.0 kPa (standard deviation was 0.8 kPa based on at least 1000 points).

2.3. Contractile force and strain energy analysis

Time lapse images of the fluorescent-labeled collagen gel surface with beating hiPSC-CMs was observed using a fluorescent microscope with a 20× objective lens (Ti-E and CFI-Plan Apo λseries; NIKON, Tokyo, Japan) and sCMOS camera (Zyla 4.2; Andor Technology Ltd., UK) at 1500 × 1500 pixels and 10 frames/s. An example of collagen deformation is shown in Supplemental movie 1. Contractile force (traction force) of hiPSC-CMs was analyzed by particle image velocimetry and Fourier transform traction cytometry method using ImageJ software plugins [20] (National Institutes of Health, Bethesda, MD, USA). Briefly, the displacement field of the collagen gel surface between the force-free image and another image was estimated by particle image velocimetry. The traction force field was obtained by deconvolution of Green's function and the displacement field from Fourier space. The regularization parameter was set at 1×10^{-8} for traction force reconstructions. Total strain energy U of the collagen gel by the hiPSC-CMs beating was evaluated using the following equation [21]:

$$U = \frac{1}{2} \int \boldsymbol{T}(x,y) \cdot \boldsymbol{u}(x,y) \mathrm{d}x\mathrm{d}y$$

where $\boldsymbol{T}$ denotes the traction force vector and $\boldsymbol{u}$ denotes the displacement vector in a laboratory frame (x, y). Analyzed displacement, traction force and local strain energy were visualized using MATLAB software. Representative total strain energy for each cell was determined as the average of the five peak values (denoted as “Max” in the Fig. 1(C)).

Supplementary video related to this article can be found at http://dx.doi.org/10.1016/j.reth.2016.02.009.

2.4. Immunofluorescent microscopy

The hiPSC-CMs were fixed with 4% formaldehyde/PBS and permeabilized with 0.5% Triton X-100/PBS. The cells were stained with specific primary and Alexa-labeled secondary antibodies (Thermo

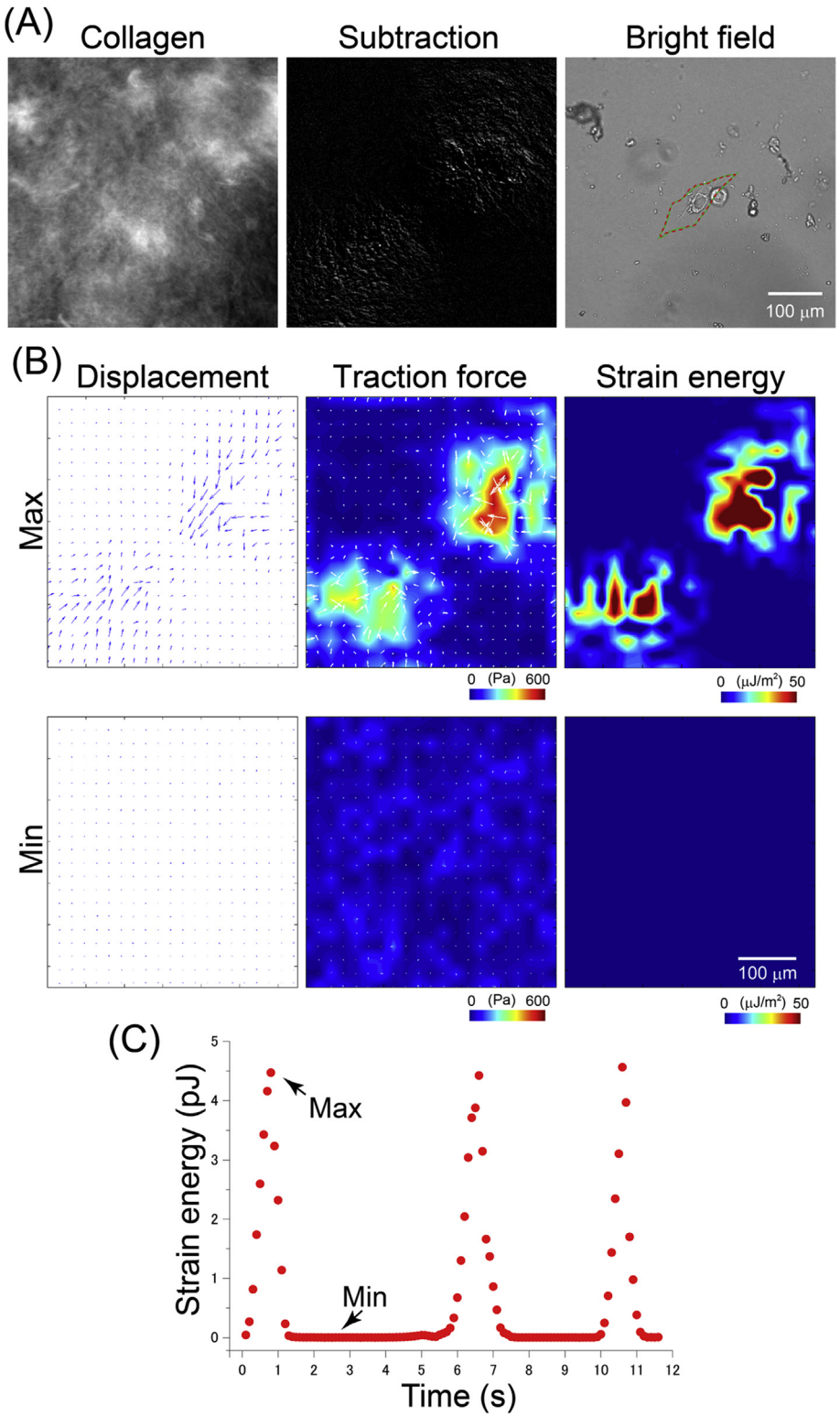

Fig. 1. Measurement and analysis of contractile force and strain energy output for a single cardiomyocyte derived from human induced pluripotent stem cells (hiPSC-CMs). Cells were cultured on a fluorescent-labeled collagen gel substrate and time lapse imaging of the beating cells was performed by fluorescent microscopy. (A) Collagen deformation caused by cell beating was captured and visualized. The "subtraction" was conducted by subtracting the two collagen images using ImageJ software. Green solid line and red dashed line indicate the cellular outline of the relaxed and contracted states, respectively. (B) Using two collagen images, we analyzed the displacement, traction force, and strain energy of the collagen gel surface. "Max" denotes the analysis using the relaxed and contracted collagen images. "Min" denotes the analysis using the two relaxed collagen images. (C) Time course of the total strain energy from a cell was plotted.

Fisher Scientific), and then washed with PBS. Information regarding the primary antibodies used in this study is presented in Supplemental data. For confocal laser microscope imaging, we used the C1 system (NIKON) with a 20×, 60×, or 100× objective lens (CFI-Plan Apo λseries; NIKON). For super resolution imaging, we used Nikon's Structured Illumination Microscope (N-SIM;

NIKON) with a 100× objective lens (Apo TIRF Oil DIC; NIKON). Image reconstruction from structured-illumination images was performed using N-SIM software.

3. Results

3.1. Variety of mechanical outputs of hiPSC-CMs

We measured the mechanical features of single hiPSC-CMs. Prior to applying single hiPSC-CMs in contractile force measurement, we observed the pulsation of hiPSC-CMs (beating cells were more than 90%) on the collagen-coated glass substrate (representative movie is shown as Supplemental movie 2). Each cell beat under the low cell-density condition. The periodicity of the beating was not uniform, but ranged from 0.2 to 1.0 Hz.

Supplementary video related to this article can be found at http://dx.doi.org/10.1016/j.reth.2016.02.009.

Next, we measured the contractile force and strain energy of isolated hiPSC-CMs. The hiPSC-CMs were cultured on fluorescent-tagged collagen gel and beating was observed (Fig. 1(A)). Displacement of the collagen gel surface, contractile force (traction force), and strain energy of single hiPSC-CMs were analyzed using a set of time-lapse images for the beating collagen gel surface (Fig. 1(B)). In the data set, the most compacted state for 5 beats was denoted as "Max" and the relaxed state was denoted as "Min". We confirmed that the distribution of collagen deformation (Fig. 1(A)) corresponded to the distribution of displacement, traction force, and strain energy in the most compacted state. To elucidate temporal changes in the strain energy output, we integrated the strain energy density for the field of the image shown in Fig. 1(B), and the time dependency of the total strain energy (plane integration of strain energy density) was plotted as shown in Fig. 1(C). These results showed that our experimental system and analysis were effective for evaluating the strain energy output of single hiPSC-CMs.

To observe cellular variations in contractility, we analyzed the distribution of representative values of total strain energy. First, we considered the validity of the representative value of total strain energy. The representative value was determined as the average of 5 peak values. To examine whether the representative value changed during cellular activity, we measured the total strain energy of three cells at a 24 h interval and compared their changes (Fig. 2(A)). Standard deviations for each data point were less than 20% of the average. There was no clear difference in the average strain energy during the 24 h cell cultivation. This indicates that the average strain energy of each cell can be considered as a representative value. Next, we measured the total strain energy of single hiPSC-CMs and plotted their representative values on a histogram (Fig. 2(B)). The total strain energy of each cell was not uniform, but ranged from 0.2 to 5.8 pJ. These results suggest that mechanical outputs from single hiPSC-CMs were not uniform, but differed between cells.

3.2. Heterogeneous filament networks of myosin II isoforms

To address the molecular mechanism of the varying strain energy output between cells, we determined the relationship between stain energy output and the fibrous distribution of MRLC isoforms, such as cardiac (contributes to beating) and non-cardiac (does not concern beating) MRLC. Strain energy on the fluorescent-labeled collagen gel was measured, and then the cells were fixed and stained with specific antibodies for the cardiac and non-cardiac MRLC. The cells showing high strain energy output (greater than 4 pJ) generally exhibited weak non-cardiac MRLC fibers (Fig. 3(A)). The cells showing low strain energy output (less than 2 pJ) generally exhibited strong non-cardiac MRLC fibers (Fig. 3(B)). However, we identified no specific features from the cardiac MRLC signals. These results suggest that strain energy output related to the degree of the non-cardiac myosin II fibers.

Next, we observed the detailed filament networks of myosin II isoforms in hiPSC-CMs by confocal laser microscopy (Fig. 4) or super resolution microscopy (Supplemental data). Localization of cardiac and non-cardiac MRLC was different, forming heterogeneous filaments rather than a filament consisting of cardiac and non-cardiac (arrows and arrowheads in Fig. 4). The filament network of cardiac MRLC included some straight and curved areas. To consider the validity of the curved fiber, we observed the localization of cardiac muscle actin using a specific antibody (Supplemental data).We observed forming curved actin fiber networks such as in cardiac MRLC localization. These results indicate that cardiac and non-cardicac MRLC constructed heterogeneous fiber networks.

To determine whether cardiac MRLC can be used as a substitute for non-cardiac MRLC, GFP-tagged cardiac MRLC was expressed with the human fibroblast cell line (MRC-5) and in hiPSC-CMs (Fig. 5). In fibroblast cells, GFP signals were diffused in the cytoplasm and nucleus. In contrast, GFP signals formed fibers in hiPSC-CMs. We also observed that hiPSC-CMs expressing the GFP-tagged cardiac MRLC can beat (Supplemental movie 3). These results indicate that cardiac and non-cardicac MRLC formed functionally different fiber networks in different locations.

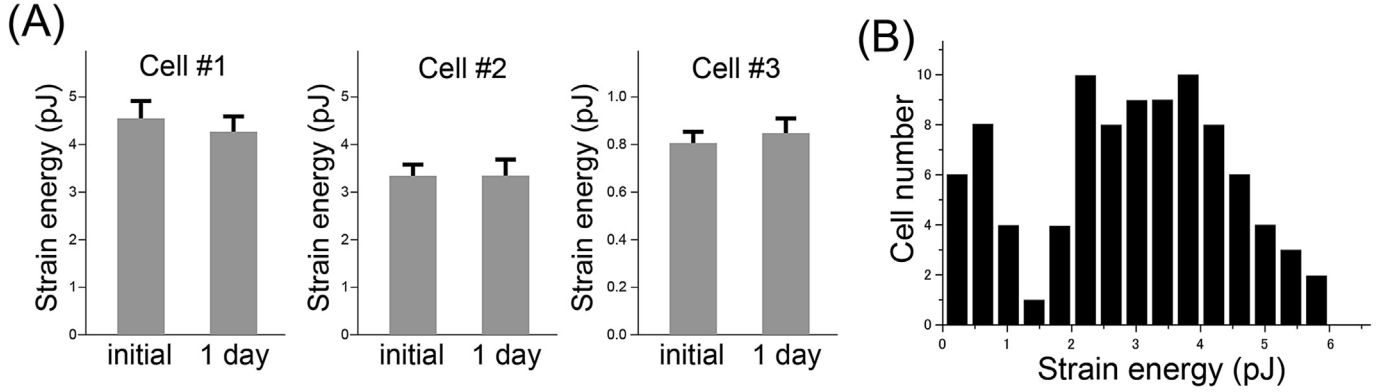

Fig. 2. Cell-dependent difference in the strain energy output. (A) Temporal changes in the total strain energy of three cells were evaluated. The five peaks of the total strain energy from a single cell were averaged (peak denotes "Max" in Fig. 1(C)). The analysis was performed again after 24 h cultivation. Temporal changes in the averaged strain energy from a cell were very small, although the average strain energy differed between the three cells. Error bars denote standard deviation. (B) Total strain energy from 92 cells (before 24 h cultivation mentioned in the Fig. 2(A)) was averaged and plotted in the histogram. Strain energy output was non-uniformly distributed between cells.

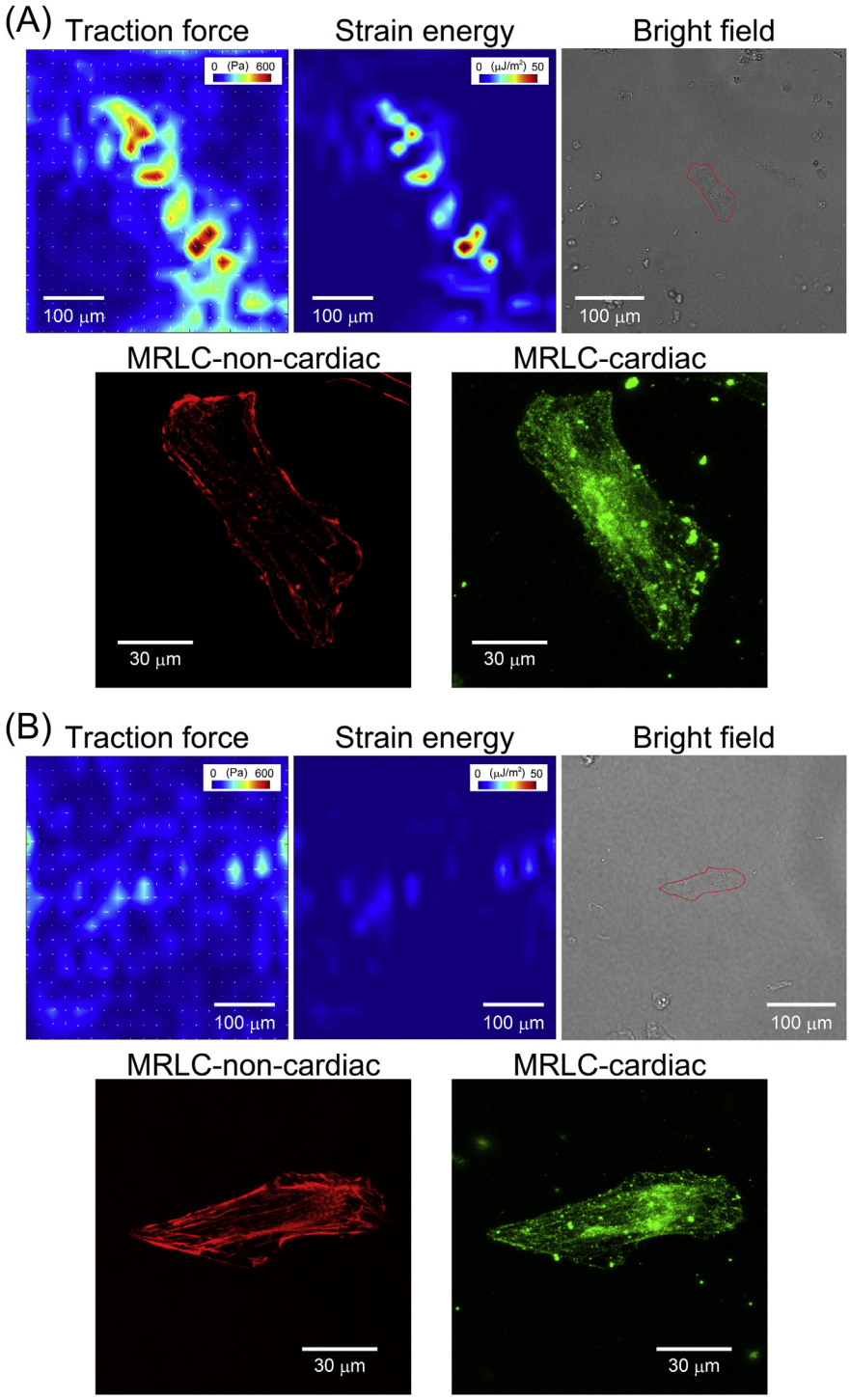

Fig. 3. Relationship between strain energy output and myosin II isoform expression. Cardiomyocytes derived from human induced pluripotent stem cells (hiPSC-CMs) were cultured on the collagen gel. Traction force and total strain energy of the cells were measured. Next, the cells were fixed and stained with antibodies for the cardiac isoform of myosin II regulatory light chain (MRLC) and non-cardiac isoform of MRLC. Red lines in the bright field image show cellular outlines. Representative data for the high energy cell (A) and low energy cell (B) are shown.

Supplementary video related to this article can be found at http://dx.doi.org/10.1016/j.reth.2016.02.009.

4. Discussion

In this study, we showed that the contractile force and strain energy output of hiPSC-CMs were non-uniformly distributed between cells (Fig. 2). Although the collagen gel was not uniform (Fig. 1(A) and the elasticity distribution measured by AFM), the distribution of elasticity was not sufficient for the broad distribution of strain energy output by hiPSC-CMs (Fig. 2(B)). Cells showing high strain energy output generally contained weak non-cardiac myosin II fibers and vice versa (Fig. 3). Cardiac myosin II and non-cardiac myosin II formed heterogeneous fiber networks (Fig. 4).

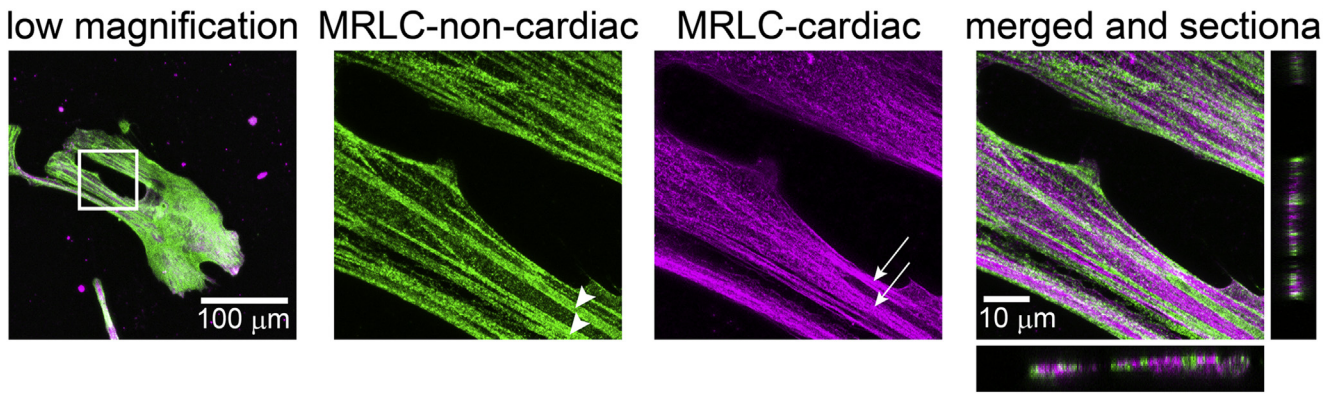

Fig. 4. Myosin II isoforms constructed heterogeneous filament networks. Cardiomyocytes derived from human induced pluripotent stem cells (hiPSC-CMs) were cultured on the glass substrate, fixed and stained with specific antibodies for the cardiac isoform of myosin II regulatory light chain (MRLC) and non-cardiac isoform of MRLC. Immunofluorescent images were acquired by confocal laser microscopy with a 20× or 100× objective lens. Representative cells are shown. The arrows and arrowheads indicate the different fiber networks.

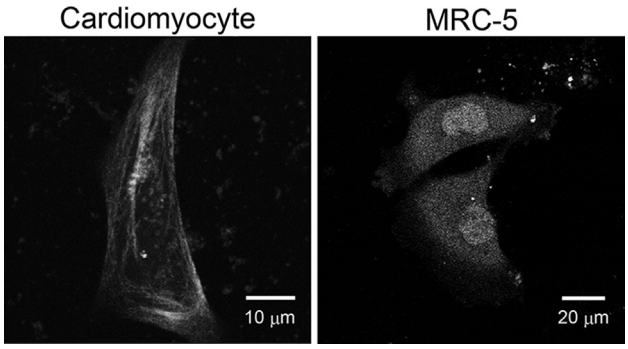

Fig. 5. Cardiac isoform of myosin II regulatory light chain (MRLC) could not substitute for the non-cardiac isoform of MRLC. A plasmid for the GFP-tagged cardiac MRLC was transfected into cardiomyocytes derived from human induced pluripotent stem cells (hiPSC-CMs) and the human fibroblast cell line (MRC-5). The localization of GFP signals was compared.

Regardless of whether the heterogeneous fiber networks showed the same alignment, the beating component (cardiac myosin II fibers) contributed to the generation of the beating force, while the non-beating component (non-cardiac myosin II fibers) resisted beating force through its elasticity. Considering this, we confirmed that non-cardiac myosin II fibers networks functioned as an elastic material and weakened the contractile force and energy output of hiPSC-CMs.

The reason why the degree of non-cardiac myosin II fibers formations differed between cells remains unclear. Differences in the maturation of hiPSC-CMs may affect non-cardiac myosin II fiber formation. The maturation of hiPSC-CMs changes some cardio-related protein [22] and alters cellular morphologies and functions [23]. As the maturation process slightly differs between cells, expression in non-cardiac myosin II may be affected. Non-cardiac MRLC expression in cardiomyocytes is not unusual, because one type of non-cardiac MRLC (myosin, light chain 12A, NM_006471) is expressed in the heart at the same level as in the muscle according to the GeneChip database (http://refex.dbcls.jp/index.php). Expression may be regulated in the unique manner exhibited by induced pluripotent stem cells.

To obtain high contractile-force hiPSC-CMs, in addition to the cell sorting using specific protein markers, genomic manipulation or cell sorting based on cellular mechanical properties is required. To differentially regulate cardiac and non-cardiac myosin II, a cardiac myosin II-specific regulator [24] is one target of genomic manipulation. Cell sorting depending on mechanical properties such as cellular stiffness [25] should also be examined.

Conflict of interest

All authors declare no conflict of interest associated with this manuscript.

Acknowledgment

We would like to thank Toru Imase (NIKON), Kazuaki Tokunaga (NIKON) and Kentarou Kobayashi (Nikon Imaging Center at Hokkaido University) for their technical supports with N-SIM observation. This study was supported by the Grant-in-Aid for Challenging Exploratory Research (15K15010) and Scientific Research on Innovative Areas (26106704) to T.M., and Scientific Research on Innovative Areas (26106703) to K.F., and Scientific Research on Innovative Areas (15H05858) to H.H. and Scientific Research (B) (25287106) to K.K. from the Ministry of Education, Culture, Sports, Science, and Technology, Japan.

Appendix A. Supplementary data

Supplementary data related to this article can be found at http://dx.doi.org/10.1016/j.reth.2016.02.009.

References

[1] Sahara M, Santoro F, Chien KR. Programming and reprogramming a human heart cell. EMBO J 2015;34:710–38.
[2] Feric NT, Radisic M. Maturing human pluripotent stem cell-derived cardiomyocytes in human engineered cardiac tissues. Adv Drug Deliv Rev 2015;96:110–738.
[3] Schwan J, Campbell SG. Prospects for in vitro myofilament maturation in stem cell-derived cardiac myocytes. Biomark Insights 2015;10:91–103.
[4] Lu TY, Lin B, Kim J, Sullivan M, Tobita K, Salama G, et al. Repopulation of decellularized mouse heart with human induced pluripotent stem cell-derived cardiovascular progenitor cells. Nat Commun 2013;4:2307.
[5] Uosaki H, Fukushima H, Takeuchi A, Matsuoka S, Nakatsuji N, Yamanaka S, et al. Efficient and scalable purification of cardiomyocytes from human embryonic and induced pluripotent stem cells by VCAM1 surface expression. PLoS One 2011;6:e23657.
[6] Masumoto H, Ikuno T, Takeda M, Fukushima H, Marui A, Katayama S, et al. Human iPS cell-engineered cardiac tissue sheets with cardiomyocytes and vascular cells for cardiac regeneration. Sci Rep 2014;4:6716.
[7] Hayakawa T, Kunihiro T, Ando T, Kobayashi S, Matsui E, Yada H, et al. Image-based evaluation of contraction-relaxation kinetics of human-induced pluripotent stem cell-derived cardiomyocytes: correlation and complementarity with extracellular electrophysiology. J Mol Cell Cardiol 2014;77:178–91.

[8] Ribeiro AJ, Ang YS, Fu JD, Rivas RN, Mohamed TM, Higgs GC, et al. Contractility of single cardiomyocytes differentiated from pluripotent stem cells depends on physiological shape and substrate stiffness. Proc Natl Acad Sci U S A 2015;112:12705–10.
[9] Rodriguez ML, Graham BT, Pabon LM, Han SJ, Murry CE, Sniadecki NJ. Measuring the contractile forces of human induced pluripotent stem cell-derived cardiomyocytes with arrays of microposts. J Biomech Eng 2014;136:051005.
[10] Sugiura S, Nishimura S, Yasuda S, Hosoya Y, Katoh K. Carbon fiber technique for the investigation of single-cell mechanics in intact cardiac myocytes. Nat Protoc 2006;1:1453–7.
[11] Mizutani T, Takeda K, Haga H, Todo M, Kawabata K. Modulation of extracellular conditions prevents the multilayering of the simple epithelium. Histochem Cell Biol 2014;141:473–81.
[12] Lee B, Zhou X, Riching K, Eliceiri KW, Keely PJ, Guelcher SA, et al. A three-dimensional computational model of collagen network mechanics. PLoS One 2014;9:e111896.
[13] Schillers H, Walte M, Urbanova K, Oberleithner H. Real-time monitoring of cell elasticity reveals oscillating myosin activity. Biophys J 2010;99:3639–46.
[14] Nagayama M, Haga H, Takahashi M, Saitoh T, Kawabata K. Contribution of cellular contractility to spatial and temporal variations in cellular stiffness. Exp Cell Res 2004;300:396–405.
[15] Mizutani T, Li R, Haga H, Kawabata K. Transgene integration into the human AAVS1 locus enhances myosin II-dependent contractile force by reducing expression of myosin binding subunit 85. Biochem Biophysical Res Commun 2015;465:270–4.
[16] Yamato M, Adachi E, Yamamoto K, Hayashi T. Condensation of collagen fibrils to the direct vicinity of fibroblasts as a cause of gel contraction. J Biochem 1995;117:940–6.
[17] Sun W, Lim CT, Kurniawan NA. Mechanistic adaptability of cancer cells strongly affects anti-migratory drug efficacy. J R Soc Interface 2014;11.
[18] Roeder BA, Kokini K, Sturgis JE, Robinson JP, Voytik-Harbin SL. Tensile mechanical properties of three-dimensional type I collagen extracellular matrices with varied microstructure. J Biomech Eng 2002;124:214–22.
[19] Mizutani T, Haga H, Kato K, Matsuda K, Kawabata K. Observation of stiff domain structure on collagen gels by wide-range scanning probe microscopy. Jpn J Appl Phys 2006;45:2353–6.
[20] Tseng Q, Duchemin-Pelletier E, Deshiere A, Balland M, Guillou H, Filhol O, et al. Spatial organization of the extracellular matrix regulates cell-cell junction positioning. Proc Natl Acad Sci U S A 2012;109:1506–11.
[21] Butler JP, Tolic-Norrelykke IM, Fabry B, Fredberg JJ. Traction fields, moments, and strain energy that cells exert on their surroundings. Am J Physiol Cell Physiol 2002;282:C595–605.
[22] Bedada FB, Chan SS, Metzger SK, Zhang L, Zhang J, Garry DJ, et al. Acquisition of a quantitative, stoichiometrically conserved ratiometric marker of maturation status in stem cell-derived cardiac myocytes. Stem Cell Rep 2014;3:594–605.
[23] Lundy SD, Zhu WZ, Regnier M, Laflamme MA. Structural and functional maturation of cardiomyocytes derived from human pluripotent stem cells. Stem Cells Dev 2013;22:1991–2002.
[24] Chan JY, Takeda M, Briggs LE, Graham ML, Lu JT, Horikoshi N, et al. Identification of cardiac-specific myosin light chain kinase. Circ Res 2008;102:571–80.
[25] Hirose YT, Higashimori K, Arai M, Kaneko T, Iitsuka M, Yamanishi R, et al. A new stiffness evaluation toward high speed cell sorter. In: 2010 IEEE international conference on robotics and automation anchorage convention district; 2010. p. 4113–8.